

# Bi-collinear antiferromagnetic order in the tetragonal $\alpha$ -FeTe

Fengjie Ma<sup>1,3</sup>, Wei Ji<sup>3</sup>, Jiangping Hu<sup>2</sup>, Zhong-Yi Lu<sup>3,\*</sup> and Tao Xiang<sup>4,1†</sup>

<sup>1</sup>*Institute of Theoretical Physics, Chinese Academy of Sciences, Beijing 100190, China*

<sup>2</sup>*Department of Physics, Purdue University, West Lafayette, Indiana 47907, USA*

<sup>3</sup>*Department of Physics, Renmin University of China, Beijing 100872, China and*

<sup>4</sup>*Institute of Physics, Chinese Academy of Sciences, Beijing 100190, China*

(Dated: November 20, 2018)

By the first-principles electronic structure calculations, we find that the ground state of PbO-type tetragonal  $\alpha$ -FeTe is in a bi-collinear antiferromagnetic state, in which the Fe local moments ( $\sim 2.5\mu_B$ ) are ordered ferromagnetically along a diagonal direction and antiferromagnetically along the other diagonal direction on the Fe square lattice. This bi-collinear order results from the interplay among the nearest, next nearest, and next next nearest neighbor superexchange interactions  $J_1$ ,  $J_2$ , and  $J_3$ , mediated by Te 5p-band. In contrast, the ground state of  $\alpha$ -FeSe is in the collinear antiferromagnetic order, similar as in LaFeAsO and BaFe<sub>2</sub>As<sub>2</sub>.

PACS numbers: 74.25.Jb, 71.18.+y, 74.70.-b, 74.25.Ha, 71.20.-b

The recent discovery of superconductivity in the layered iron-based compounds attracts great interest, not only because the second highest superconductivity temperatures are achieved, but also because it is the first time that Fe atoms directly play an important role in superconductivity while the Fe atoms are conventionally considered in disfavor of superconductivity. Until now there are four types of iron-based compounds that have been reported to show superconductivity when doping or under high pressures. They are classified as ‘1111’ type (prototype: LaFeAsO [1]), ‘122’ type (prototype: BaFe<sub>2</sub>As<sub>2</sub> [2]), ‘111’ type (prototype: LiFeAs [3]), and ‘11’ type (prototype: tetragonal  $\alpha$ -FeSe(Te) [4, 5]). The common feature shared by these compounds is that there are the robust tetrahedral layers where Fe atoms are tetragonally coordinated by pnictide or chalcogenide atoms and the superconduction pairing happens on these layers.

It has been found that for both ‘1111’ and ‘122’ compounds there happens a tetragonal-orthorhombic structural phase transition [6]. For undoped ‘1111’, about 15K below this structural transition, a magnetic phase transition takes place while for undoped ‘122’ compounds, the structural and magnetic phase transitions occur at the same temperature. The magnetic order associated with the transition is a collinear antiferromagnetic order. The microscopic mechanisms underlying the structural transition and antiferromagnetic transition and the relationship between these two transitions have been centered in hot debate. There are two very different microscopic pictures in understanding the phase transitions. The first one suggests that there are no local moments and the collinear antiferromagnetic order is entirely induced by the Fermi surface nesting which is also likely responsible for the structural transition due to breaking the four-fold rotational symmetry [7, 8]. The second one suggests that As-bridged superexchange antiferromagnetic interactions between the nearest neighbor and next nearest

neighbor Fe-Fe fluctuating local moments are the driving force upon the two transitions [9, 10, 11].

In this letter, we report the electronic structure calculations on tetragonal  $\alpha$ -FeTe and  $\alpha$ -FeSe. We find that the ground state of  $\alpha$ -FeTe is in a bi-collinear antiferromagnetic order as schematically shown in Fig. 1(a), which differs from the collinear antiferromagnetic order. The underlying physics of this magnetic ordering can be described well in a model with the magnetic exchange interactions  $J_1$ ,  $J_2$ , and  $J_3$  respectively between the nearest, next nearest, and next next nearest neighbor mediated by Te-5p band (Fig. 1(a)). Hence, the fluctuating local moment picture works well in understanding the magnetism while the magnetic order can not be easily obtained from the Fermi Surface nesting picture. In the bi-collinear antiferromagnetic state, the bi-collinear antiferromagnetic ordering is along the diagonal direction of the Fe-Fe square lattice with double collinearity. If the Fe-Fe square lattice is divided into two square sublattices A and B shown in Fig. 1(a), the Fe moments on each Fe-Fe sublattice take its own collinear antiferromagnetic order. Our results are in excellent agreement with neutron experimental results [12, 13]. In contrast, the ground state of tetragonal  $\alpha$ -FeSe is a conventional collinear antiferromagnetic state, similar to LaFeAsO and BaFe<sub>2</sub>As<sub>2</sub>.

In the calculations the plane wave basis method was used [14]. We employed the local (spin) density approximation and the generalized gradient approximation of Perdew-Burke-Ernzerhof [15] for the exchange-correlation potentials. The ultrasoft pseudopotentials [16] were used to model the electron-ion interactions. After the full convergence test, the kinetic energy cut-off and the charge density cut-off of the plane wave basis were chosen to be 800eV and 6400eV, respectively. The Gaussian broadening technique was used and a mesh of  $18 \times 18 \times 9$  k-points were sampled for the Brillouin-zone integration. In the calculations, the internal atomic coordinates within the cell were determined by the energy min-

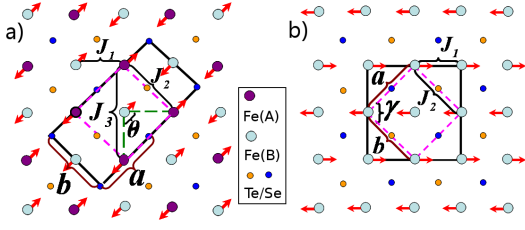


FIG. 1: (Color online) Schematic top view of the FeTe (FeSe) layer. The ordered Fe spins are shown by red arrows. The small dashed square is an  $a \times b$  ( $a = b$ ) unit cell. (a) bi-collinear ordering with a  $2a \times b$  as the unit cell shown by solid rectangle; (b) collinear ordering with a  $\sqrt{2}a \times \sqrt{2}b$  as the unit cell shown by solid square.

imization. Among all the four types of iron-based compounds,  $\alpha$ -FeSe and  $\alpha$ -FeTe possess the simplest structure, made up only of two kinds of atoms Fe and Se or Te. They consist of continuous stacking of tetrahedral FeSe or FeTe layers along  $c$ -axis without any other kind of layers.  $\alpha$ -FeSe and  $\alpha$ -FeTe belong to a tetragonal family with  $PbO$ -type structure and space group of  $P4/nmm$ . The experimental tetragonal lattice parameters were adopted in our calculations [4, 5, 12, 13, 17].

Our nonmagnetic calculations on both  $\alpha$ -FeSe and  $\alpha$ -FeTe exclude any possible structural distortions like Jahn-Teller effect. This means that a structural distortion on  $\alpha$ -FeSe or  $\alpha$ -FeTe if existing is very likely driven by magnetic forces. The calculated nonmagnetic electronic energy band structures and Fermi surfaces are the same as those reported in Ref. [18].

Now let's consider possible magnetic orders. If we divide the Fe-Fe square lattice into two square sublattices  $A$  and  $B$ , there may be ferromagnetic, square antiferromagnetic, or collinear antiferromagnetic order for the Fe moments on each of the two sublattices. The combination of these magnetic orders on the two sublattices yield the ferromagnetic, square antiferromagnetic, collinear antiferromagnetic, and bi-collinear antiferromagnetic orders on the Fe-Fe square lattice, as shown in Fig. 1. To calculate the bi-collinear antiferromagnetic order and collinear antiferromagnetic order, we adopt  $2a \times a \times c$  and  $\sqrt{2}a \times \sqrt{2}a \times c$  unit cells, respectively shown in Fig. 1(a) and (b). For the other magnetic orders, the  $a \times a \times c$  unit cell is used.

If the energy of the nonmagnetic state is set to zero, through the calculations we find that the energies of the ferromagnetic ( $E_{FE}$ ), square antiferromagnetic ( $E_{AFM}$ ), collinear antiferromagnetic ( $E_{COL}$ ), and bi-collinear antiferromagnetic states ( $E_{BI}$ ) are (0.183, -0.101, -0.0152, -0.089) eV/Fe for  $\alpha$ -FeSe and (-0.0897, -0.0980, -0.156, -0.166) eV/Fe for  $\alpha$ -FeTe, respectively. Thus the ground state of  $\alpha$ -FeSe is a collinear-ordered antiferromagnetic state, similar to LaFeAsO and BaFe<sub>2</sub>As<sub>2</sub>. In contrast, the ground stat of  $\alpha$ -FeTe is a bi-collinear ordered antifer-

romagnetic state, being lower in energy by  $\sim 10$  meV/Fe than its collinear ordered antiferromagnetic state.

The magnetic moment located around each Fe atom is found to be about  $2.2 \sim 2.6 \mu_B$ , similar to the cases of LaFeAsO and BaFe<sub>2</sub>As<sub>2</sub>, varying weakly in the above four magnetically ordered states. Since these local moments are embedded in the environment of itinerant electrons, the moment of Fe ions is fluctuating. Nevertheless, we may here reasonably consider the spin of Fe ions is equal to 1. But the corresponding long range ordered moment should be smaller because the correlated effect, especially the strong competition between different antiferromagnetic states, has not been fully included in the density functional theory calculation.

To quantify the magnetic interactions, we assume that the energy differences between these magnetic orderings are predominantly contributed from the interactions between the Fe spins ( $S = 1$ ), which can be modeled by the following frustrated Heisenberg model with the nearest, next-nearest, and next next nearest neighbor couplings  $J_1$ ,  $J_2$ , and  $J_3$ ,

$$H = J_1 \sum_{\langle ij \rangle} \vec{S}_i \cdot \vec{S}_j + J_2 \sum_{\langle\langle ij \rangle\rangle} \vec{S}_i \cdot \vec{S}_j + J_3 \sum_{\langle\langle\langle ij \rangle\rangle\rangle} \vec{S}_i \cdot \vec{S}_j, \quad (1)$$

whereas  $\langle ij \rangle$ ,  $\langle\langle ij \rangle\rangle$  and  $\langle\langle\langle ij \rangle\rangle\rangle$  denote the summation over the nearest, the next-nearest and the next-next-nearest neighbors, respectively. Since both  $\alpha$ -FeSe and FeTe are semimetals, the above modeling may miss the certain contribution from the itinerant electrons. However we believe that the above simply modeling captures the substantial physics on the magnetic structures. From the calculated energy data, we find that for  $\alpha$ -FeTe  $J_1 = 2.1 \text{ meV}/S^2$ ,  $J_2 = 15.8 \text{ meV}/S^2$ , and  $J_3 = 10.1 \text{ meV}/S^2$  while for  $\alpha$ -FeSe  $J_1 = 71 \text{ meV}/S^2$ ,  $J_2 = 48 \text{ meV}/S^2$ , and  $J_3 = 8.5 \text{ meV}/S^2$ . Notice that the ferromagnetic state is quite low in energy in  $\alpha$ -FeTe, which is reason why  $J_1$  is so small.

It is well-known that for a  $J_1$ - $J_2$  antiferromagnetic square lattice the frustration between  $J_1$  and  $J_2$  will destruct the Neel state and induce a collinear antiferromagnetic order when  $J_2 > J_1/2$  as shown in Fig. 1(b), in which we notice that each site spin has two ferromagnetic connection neighbors and two antiferromagnetic connection neighbors. Further inspection of Fig. 1 shows that  $J_2$  and  $J_3$  are the nearest and the next-nearest couplings for each of sublattice A and B whereas  $J_1$  is the connection coupling between A and B. When  $J_3 > J_2/2$  and  $2J_2 + 4J_3 > J_1$  [19], a collinear antiferromagnetic ordering will take place on each sublattice. It turns out that the bi-collinear antiferromagnetic ordering occurs on the square lattice as shown in Fig. 1(a), in which we notice again that each site spin has two ferromagnetic connection neighbors and two antiferromagnetic connection neighbors that doesn't cost more energy on  $J_1$  in comparison with the collinear antiferromagnetic order. Overall,

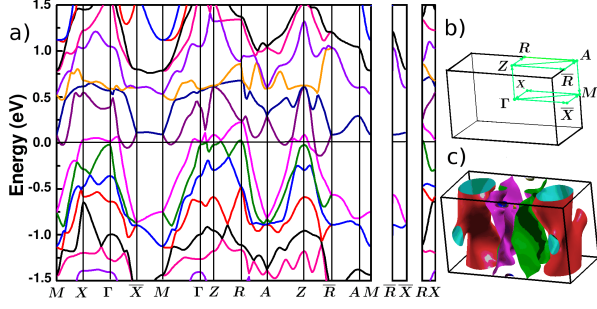


FIG. 2: (Color online) (a) Electronic band structure of the bi-collinear-ordered antiferromagnetic  $\alpha$ -FeTe. The Fermi energy is set to zero. (b) Brillouin zone. (c) Fermi surface.  $\Gamma\bar{X}$  ( $\Gamma X$ ) corresponds to the parallel(antiparallel)-aligned moment line.

when  $J_3 > J_2/2$  and  $J_2 > J_1/2$ , by recursion we may thus expect that a bi-collinear antiferromagnetic state would be the ground state of the frustrated  $J_1$ - $J_2$ - $J_3$  Heisenberg model (1), which is in good agreement with the derived  $J_1$ ,  $J_2$ , and  $J_3$  on  $\alpha$ -FeTe and  $\alpha$ -FeSe. Especially, we can show that  $J_3 = J_2/2 + (E_{COL} - E_{BI})/4S^2$  and  $J_2 = J_1/2 + (E_{AFM} - E_{COL})/4S^2$  [21]. The energy ordering is  $E_{FM} > E_{AFM} > E_{COL} > E_{BI}$  for  $\alpha$ -FeTe and  $E_{FM} > E_{BI} > E_{AFM} > E_{COL}$  for  $\alpha$ -FeSe. By model (1) we may thus easily understand the complex magnetic structures displayed by  $\alpha$ -FeTe and  $\alpha$ -FeSe.

When we further consider the possible spin-phonon interaction, it is expected that there would be further lattice relaxation, similar to spin-Peierls distortion, that is, being slightly longer along spin anti-parallel alignment to further favor antiferromagnetic energy and shorter along spin parallel alignment to further favor ferromagnetic energy. Correspondingly,  $\theta$  and  $\gamma$  increase slightly respectively for the bi-collinear and collinear cases (Fig. 1(a) and (b)). As a matter of fact, we indeed find such extra small structural distortions for both  $\alpha$ -FeTe and  $\alpha$ -FeSe. For  $\alpha$ -FeTe,  $\theta$  increases to  $92.03^\circ$  with an extra energy gain of  $\sim 5$  meV/Fe while for  $\alpha$ -FeSe,  $\gamma$  increases to  $90.5^\circ$  with an extra energy gain of  $\sim 2$  meV/Fe. As results, the crystal unit cell of  $\alpha$ -FeTe ( $\alpha$ -FeSe) on FeTe (FeSe) layer deforms from a square to a rectangle (rhombus), as shown in Fig. 1. However, we find that this small lattice distortion affects weakly the electronic band structure and the Fe moments.

Our calculations also show that for both  $\alpha$ -FeTe and  $\alpha$ -FeSe the Fe magnetic moments between the nearest neighbor layers FeTe (FeSe) prefer the anti-parallel alignment but with a small energy gain less than 1 meV/Fe, similar to LaFeAsO. It is thus very likely that here the magnetic phase transition would happen below the structural transition temperature.

Fig. 2 shows the electronic band structure and the Fermi surface of  $\alpha$ -FeTe in the bi-collinear antiferromagnetic order. There are three bands crossing the Fermi

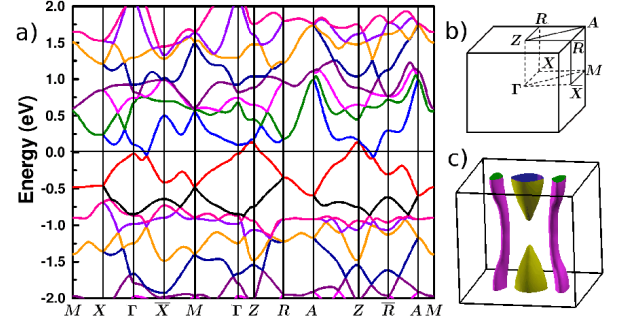


FIG. 3: (Color online) (a) Electronic band structure of the collinear-ordered antiferromagnetic  $\alpha$ -FeSe. The Fermi energy is set to zero. (b) Brillouin zone. (c) Fermi surface.  $\Gamma\bar{X}$  ( $\Gamma X$ ) corresponds to the parallel(antiparallel)-aligned moment line.

level which form three discrete parts of the Fermi surface. The Fermi surface contains a small hole-type pocket around R, two pieces of opened irregular hole-type sheets parallel to the plane  $\Gamma$ -Z-R-X, and two ‘blood vessel’-like electron-type cylinders between  $\Gamma$  and  $\bar{X}$ . From the volumes enclosed by these Fermi surface sheets, we find that the electron (hole) carrier density is 0.43 electron/cell (0.41 hole/cell), namely,  $2.38 \times 10^{21}/\text{cm}^3$  ( $2.26 \times 10^{21}/\text{cm}^3$ ). In comparison with the nonmagnetic state, the carrier density is just reduced by half. The density of states at  $E_F$  is 1.98 state/(eV Fe), which yields the electronic specific heat coefficients  $\gamma = 4.665$  mJ/(K<sup>2</sup> \* mol).

The electronic band structure and Fermi surface of  $\alpha$ -FeSe in collinear antiferromagnetic state is shown in Fig. 3. The Fermi surface consists of three sheets formed by two bands crossing the Fermi level. Specifically, one hole-type close sheet forms a hole pocket centered around Z and the other two electron-type cylinders are formed between  $\Gamma$  and  $\bar{X}$ , crossing the Fermi level. The volumes enclosed by these sheets give the electron (hole) carrier density 0.042 electrons/cell (0.028 holes/cell), namely  $2.68 \times 10^{20}/\text{cm}^3$  ( $1.81 \times 10^{20}/\text{cm}^3$ ). In comparison with the nonmagnetic state, the carrier density is reduced by one magnitude while in LaFeAsO the corresponding reduction is more than hundred times. The density of states at  $E_F$  is 0.48 state/(eV Fe), which yields the electronic specific heat coefficients  $\gamma = 1.129$  mJ/(K<sup>2</sup> \* mol).

By projecting the density of states onto the five 3d orbitals of Fe, we find that the five up-spin orbitals are almost completely filled while the five down-spin orbitals are nearly uniformly filled by half. This indicates that the crystal field splitting imposed by Se or Te atoms is very weak and the Fe 3d-orbitals hybridize strongly with each other. As the Hund rule coupling is strong, this would lead to a large magnetic moment formed around each Fe atom, as found in our calculations. Moreover, Fig. 4 clearly shows that the band states constituted by

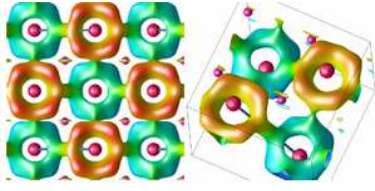


FIG. 4: (Color online) Top (left) and off-top (right) views of differential charge density for  $\alpha$ -FeSe. The isosurface value was set to  $0.03 e/\text{\AA}^3$ . Colors mapped on isosurfaces represent the relative height of data points in  $c$ -direction.

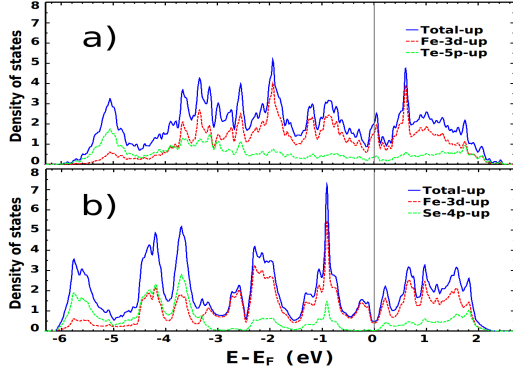


FIG. 5: (Color online) Total and orbital-resolved partial density of states (spin-up part): a) bi-collinear antiferromagnetic  $\alpha$ -FeTe; b) collinear antiferromagnetic  $\alpha$ -FeSe.

Fe 3d orbitals are very localized. Fig. 4 plots the differential charge density distribution for  $\alpha$ -FeSe ( $\alpha$ -FeTe and LaFeAsO all have similar distribution[21]). We find that the most charge accumulations are surrounding Se (Te, As) atoms (larger pink balls), while the Fe atoms (smaller red balls) only have very small charge accumulation. Figure 4 (right) further shows a differential charge density pipeline connecting from a higher Se to a lower Se. For each Se atom, there are four charge accumulation pipelines connecting from it to its four adjacent Se atoms, suggesting an electron network mostly formed by delocalized electrons of Se through covalent bonding, in which the very localized Fe electron states are embedded.

On the other hand, Fig. 5 shows that the band formed by Se 4p orbitals (also As 4p orbitals) is gapped at the Fermi energy while the band formed by Te 5p orbitals is partially filled. So there are itinerant 5p electrons at Fermi energy involved in mediating the exchange interactions in  $\alpha$ -FeTe, likely, a long-range effect. This may explain why the coupling  $J_3$  is nearly zero for  $\alpha$ -FeSe, LaFeAsO and BaFe<sub>2</sub>As<sub>2</sub>.

It was reported[4, 5] in experiment that at 105K the tetragonal  $\alpha$ -FeSe compound experiences a similar structural distortion as LaFeAsO, with  $a = b$  and  $\gamma$  changing from  $90^\circ$  to  $90.3^\circ$  while at 45K the tetragonal  $\alpha$ -FeTe compound also experiences a structural distortion but with  $a \neq b$  ( $a = 3.824 \text{ \AA}$ ,  $b = 3.854 \text{ \AA}$ ) and  $\gamma = 90^\circ$ .

This is in excellent agreement with our calculations. Furthermore, by the neutron scattering Bao and coworkers [12] found that an incommensurate antiferromagnetic order propagates along the diagonal direction of the Fe-Fe square lattice, but they also find this incommensurate ordering is easily tunable with composition and locks into a commensurate order in the metallic phase. By our calculation, it is clear that the magnetic order must be along the diagonal direction for  $\alpha$ -FeTe. A physical picture suggested in our study is that the Fe moments are mediated by Te 5p-band and the origin  $J_3$  exchange coupling may be well induced through a RKKY-type mechanism. It is very likely that the excess interstitial Fe moments drive the bi-collinear order into the incommensurate order. Notice that this diagonal antiferromagnetic order cannot be straightforwardly understood by the Fermi surface nesting picture.

In conclusion, we have presented the electronic band structure of  $\alpha$ -FeTe based on the first-principles density functional theory calculations. Our studies show that the compound  $\alpha$ -FeTe is a quasi-2-dimensional bi-collinear antiferromagnetic semimetal with a magnetic moment of  $\sim 2.5\mu_B$  around each Fe atoms.

This work is partially supported by National Natural Science Foundation of China and by National Program for Basic Research of MOST, China. JPH were supported by the NSF of US under grant No. PHY-0603759. We would like to thank P. Dai and S. Li for sharing his unpublished neutron scattering results.

\* Electronic address: zlu@ruc.edu.cn

† Electronic address: txiang@aphy.iphy.ac.cn

- [1] Y. Kamihara, T. Watanabe, M. Hirano, and H. Hosono, J. Am. Chem. Soc. **130**, 3296 (2008).
- [2] M. Rotter, M. Tegel, and D. Johrendt, Phys. Rev. Lett. **101**, 107006 (2008).
- [3] X.C.Wang, Q.Q. Liu, Y.X. Lv, W.B. Gao, L.X.Yang, R.C.Yu, F.Y.Li, and C.Q. Jin, cond-mat/0806.4688
- [4] Fong-Chi Hsu, Jiu-Yong Luo, Kuo-Wei Yeh, Ta-Kun Chen, Tzu-Wen Huang, Phillip M. Wu, Yong-Chi Lee, Yi-Lin Huang, Yan-Yi Chu, Der-Chung Yan, and Maw-Kuen Wu, cond-mat/0807.2369.
- [5] Kuo-Wei Yeh, Tzu-Wen Huang, Yi-Lin Huang, Ta-Kun Chen, Fong-Chi Hsu, Phillip M. Wu, Yong-Chi Lee, Yan-Yi Chu, Chi-Liang Chen, Jiu-Yong Luo, Der-Chung Yan, and Maw-Kuen Wu, cond-mat/0808.0474.
- [6] C. de la Cruz, *et al.*, Nature **453**, 899 (2008).
- [7] J. Dong, H. J. Zhang, G. Xu, Z. Li, G. Li, W. Z. Hu, D. Wu, G. F. Chen, X. Dai, J. L. Luo, Z. Fang and N. L. Wang, Europhysics Letters, **83**, 27006 (2008).
- [8] I. I. Mazin, D. J. Singh, M. D. Johannes, and M.-H. Du, Phys. Rev. Lett. **101**, 057003 (2008).
- [9] F. Ma and Z.-Y. Lu, Phys. Rev. B **78**, 033111 (2008).
- [10] T. Yildirim, Phys. Rev. Lett. **101**, 057010 (2008).
- [11] Chen Fang, Hong Yao, Wei-Feng Tsai, JiangPing Hu, and Steven A. Kivelson, Phys. Rev. B **77** 224509 (2008).

- [12] Wei Bao, Y. Qiu, Q. Huang, M. A. Green, P. Zajdel, M. R. Fitzsimmons, M. Zhernenkov, Minghu Fang, B. Qian, E.K. Vehstedt, Jinhu Yang, H.M. Pham, L. Spinu and Z.Q. Mao, cond-mat/0809.2058.
- [13] Shiliang Li, et al, unpublished.
- [14] P. Giannozzi et al., <http://www.quantum-espresso.org>.
- [15] J. P. Perdew, K. Burke, and M. Ernzerhof, Phys. Rev. Lett. **77**, 3865 (1996).
- [16] D. Vanderbilt, Phys. Rev. B **41**, 7892 (1990).
- [17] H. Okamoto, J. Phase Equilibria **12**, 383 (1991).
- [18] Alaska Subedi, Lijun Zhang, D.J. Singh, and M.H. Du, cond-mat/0807.4312.
- [19] J. Ferrer, Phys. Rev. B **47**, 8769 (1993).
- [20] Fengjie Ma, Zhong-Yi Lu, and Tao Xiang, cond-mat/0804.3370.
- [21] Fengjie Ma, Wei Ji, Zhong-Yi Lu, and Tao Xiang, to be published.